JOURNAL OF MATERIALS SCIENCE 27 (1992) 1608–1616

Fatigue crack growth in polymers subjected to fully compressive cyclic loads

L. PRUITT, R. HERMANN*, S. SURESH
Division of Engineering, Brown University, Providence, RI 02912, USA

It is experimentally demonstrated in this work that the application of cyclic compression loads to polymeric materials, specifically high-density polyethylene and polystyrene, results in the nucleation and propagation of stable fatigue cracks. The cracks grow at a progressively slower rate along the plane of the notch in a direction perpendicular to the far-field cyclic compression axis. The overall characteristics of this compression fatigue fracture are macroscopically similar to those seen in metals, ceramics, as well as discontinuously reinforced inorganic composites. It is reasoned that the origin of this Mode I compression fatigue effect is the generation of a zone of residual tensile stress locally in the vicinity of the notch-tip upon unloading from the maximum far-field compressive stress. The residual tensile field is generated by permanent damage arising from crazing and/or shear deformation ahead of the notch-tip. Evidence for the inducement of residual tensile stresses on the crack plane is provided with the aid of micrographs of near-tip region where crazes are observed along the plane of the crack, i.e. normal to the compression loading axis. Compression fatigue crack growth in polystyrene is also highly discontinuous in the sense that the crack remains dormant during thousands of fatigue cycles following which there is a burst of crack extension, possibly in association with fracture within the craze. This intermittent growth process in cyclic compression is analogous to the formation of discontinuous growth bands during the tension fatigue of many crazeable polymers. The exhaustion of the near-tip residual tensile field and the increase in the level of crack closure with increasing crack length cause the fatigue crack to arrest. The universal features of this phenomenon are discussed in the context of ductile and brittle, non-crystalline and crystalline, as well as monolithic and composite materials.

1. Introduction

Research into the fatigue behaviour of engineering materials has long been concerned with the effects of fully tensile or tensile–compressive cyclic loads on the initiation and growth of cracks. Such preponderance of research effort directed at fatigue under fully or partly tensile cyclic loads is a consequence of the tacit assumption that fully compressive cyclic loads generally do not lead to stable fracture. The application of fracture mechanics concepts to characterize fatigue crack growth also implicitly invokes the general notion that far-field tensile loads are primarily responsible for fatigue fracture because the faces of a crack remain closed during the application of compressive loads. Because a crack cannot propagate while it is closed, cyclic compressive loads would not be expected to dictate fracture behaviour.

There is, however, a growing body of experimental evidence for metallic materials which has unequivocally established that fully compressive cyclic loads can lead to both the initiation and growth of fatigue cracks [1–7]. Specifically, it has been shown that the application of compression fatigue loads to notched plates of ductile solids can cause a Mode I fatigue crack to initiate along the plane of the notch in a direction normal to the far-field compression axis. The cracks propagate at a progressively decreasing rate before arresting completely. The origin of this fatigue crack is the creation of a zone of residual tensile stresses within the cyclic plastic zone generated at the notch tip on unloading from the far-field compressive stress. Furthermore, it is also known that the periodic or random application of compressive overloads to a tension- or compression-fatigue crack can lead to an acceleration in the rate of fracture [8, 9].

Recent experimental work has established that brittle solids, such as ceramics and ceramic composites, which are not susceptible to marked levels of stable fatigue crack growth at room temperature due to the paucity of plastic deformation, also exhibit Mode I crack growth when subjected to fully compressive cyclic loads [10, 11]. Here, the growth of a

* *Permanent address*: Faculty of Technology, The Open University, Milton Keynes MK7 6AA, UK.

0022–2461

crack along the plane of a notch, in a direction normal to the far-field compression axis, arises from the creation of a cyclic damage zone at the notch tip, which is embedded within the region of intense deformation. Within the cyclic damage zone, residual tensile stresses are generated on unloading from far-field compression stress. This deformation zone can be created by such diverse mechanistic processes as microcracking, martensitic transformation, interfacial sliding or creep [11]. A particularly noteworthy feature of cyclic compression crack growth in notched plates is that both brittle and ductile solids with vastly different deformation mechanisms exhibit apparently similar Mode I crack growth as a result of the creation of reversed-zone deformation. This universal feature among diverse material systems is an outcome of the fact that residual tensile stresses, which are responsible for compression fatigue crack growth, are localized to the notch tip region so that crack growth is stable even in brittle solids at room temperature [11]. Experiments also show that in many brittle solids, such as metal–matrix composites, ceramics and ceramic–matrix composites with stress concentrations, it is often easier to initiate a stable fatigue crack in cyclic compression than in cyclic tension [11].

Although the topics of initiation and growth of cracks under fully compressive cyclic loads have received considerable attention in the recent past in the metallurgy and ceramics literature, similar studies have not been attempted on polymeric materials. Indeed, structural components made of polymers do contain stress concentrations and they are invariably subjected to cyclic compressive loads. The role of cyclic compressive loads in promoting undesirable levels of subcritical crack growth is a subject of utmost concern in the fatigue design of engineering plastics. In fact, there is existing evidence which indicates that some polymers and polymeric composites exhibit significantly lower fatigue lives in tension–compression or fully compressive cyclic loads than in cyclic tension [12].

In a preliminary investigation conducted as part of the present research work, Suresh and Pruitt [13] demonstrated that the application of fully compressive cyclic loads to notched plates of high density polyethylene and polystyrene can result in stable Mode I fracture. In this paper we provide full details on these experiments and present further results on the characteristics of fatigue crack initiation and growth in polymers subjected to fully compressive cyclic loads. Crack growth mechanisms under far-field cyclic compression are compared and contrasted with those seen under cyclic tension. Furthermore, the characteristics of compression fatigue fracture in polymers are examined in the light of similar effects seen in metals and ceramics, and the conditions for the apparent similarity are described. Experimental results of fatigue crack growth and craze formation at the crack-tip in a direction normal to the far-field cyclic compression axis are also presented to substantiate the argument that localized tensile stresses are induced in the vicinity of the advancing compression fatigue crack.

2. Experimental procedure

The principal material selected for this investigation is a high-density polyethylene. This polymer was procured in plate form (250 mm × 250 mm × 4.6 mm).

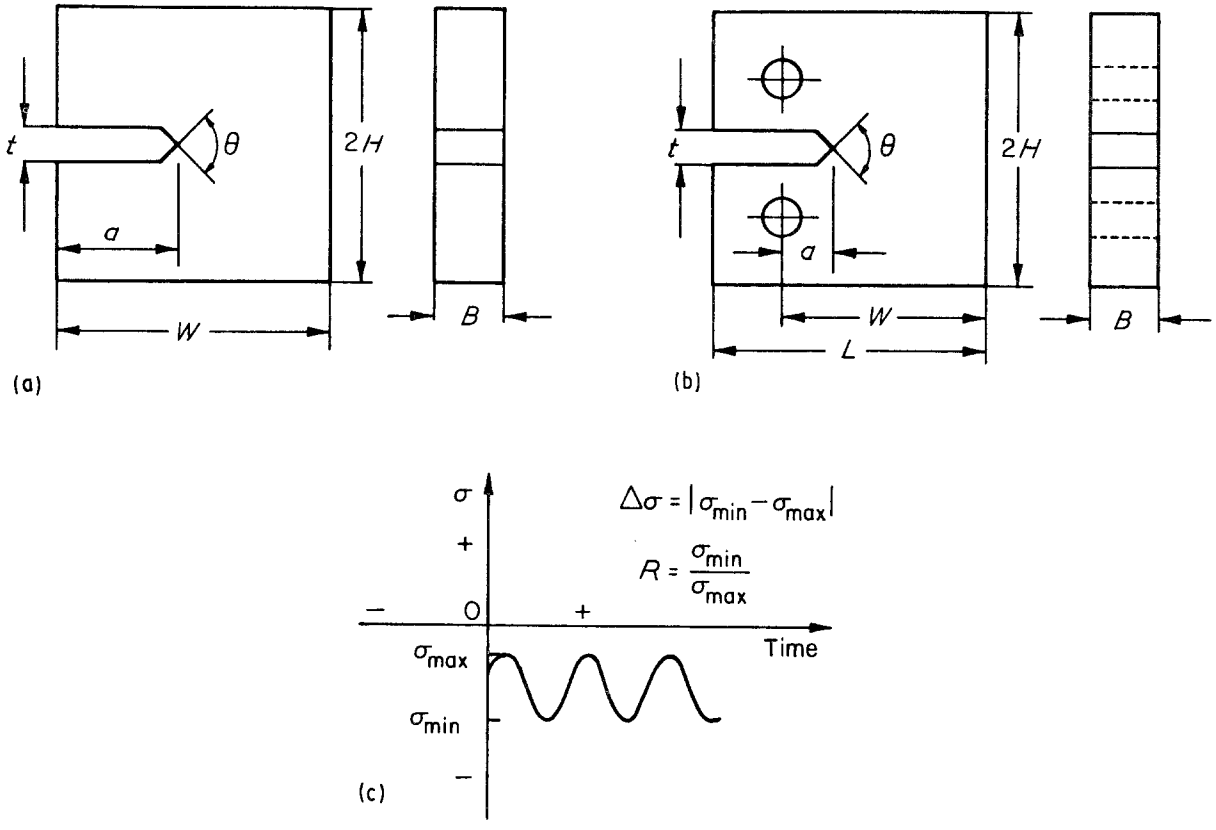

Figure 1 Schematic drawing of geometry and dimensions of (a) SEN specimen, (b) compact specimen; (c) nomenclature associated with the mechanical load variables for compression fatigue.

The polymer was analysed for crystallinity, density and molecular weight by Broutman Incorporated, Chicago, IL. The degree of crystallinity was determined to be 78% and the density of the material was 0.9669 kg m^{-3}. The weight average molecular weight, M_W, determined by gel permeation chromotography, was approximately 91 000. The physical properties of the polymer are as follows: tensile yield strength 18 MPa, ultimate tensile strength 25 MPa, and tensile modulus 0.9 GPa.

In order to illustrate the possibility of fatigue crack initiation and growth in cyclic compression, two different specimen geometries were machined from the plates for the purpose of conducting the compression fatigue experiments: a single-edge-notched specimen (SEN) and a compact specimen (C). The geometry and dimensions of the SEN specimen are shown schematically in Fig. 1a. The specimen dimensions are length $W = 19.05$ mm, height $2H = 19.05$ mm, notch length $a_0 = 5.715$ mm, thickness $B = 4.76$ mm, notch root radius $\rho = 0.127$ mm, and notch-tip angle $\theta = 45°$. The compact specimen is shown schematically in Fig. 1b. The specimen dimensions for this case are length $L = 25.4$ mm, width measured from the centre of holes $W = 19.5$ mm, height $2H = 25.4$ mm, thickness $B = 4.76$ mm, notch length $a_0 = 1.7$ mm, notch-root radius $\rho = 0.5$ mm and notch-tip angle $\theta = 60°$.

The SEN specimen was placed between two parallel surfaces which were aligned perfectly normal to the uniaxial cyclic compression loading axis in an electro-servohydrualic fatigue testing machine. (Note that any misalignment of the specimen loading surfaces from the plane normal to the loading axis will result in the growth of the crack away from the Mode I growth plane. This provides an additional check on the accuracy of the specimen alignment.) For the SEN specimen, the compressive stresses were imposed uniformly across the top and bottom surfaces. On the other hand, the compact specimen was subjected to cyclic compression loads via the loading pins. (In the case of the compact specimen, a bending moment is induced at the root of the notch which aids in the nucleation of a fatigue crack at the notch-tip; see, for example [3, 5, 6].) All experiments were conducted in the laboratory air environment at a temperature of about 23 °C and relative humidity of about 60%. The loading frequency ν was chosen to be 5 Hz (4 Hz for the compact specimens), to avoid hysteretic heating effects, with a sinusoidal waveform and a load ratio, $R = 20$ (in cyclic tension, $R = 0.1$). The load ratio, R, is defined as the ratio of minimum load to the maximum load of the fatigue cycle, $R = P_{min}/P_{max}$. The magnitude of the compressive stresses imposed on the specimen and the crack growth characteristics are discussed in the next section.

For compression fatigue work, the crack length was monitored using an optical travelling microscope with a resolution of better than 2 μm. Specimens were periodically taken out of the testing machine and 15–20 μm surface was removed by polishing to reveal the extent of crack growth beneath the surface. Upon completion of the fatigue tests, the specimens were overloaded to fracture. The fracture surfaces were analysed first by optical microscopy and then sputter coated with Au–Pd to be examined by scanning electron microscopy (SEM). The post-fracture observations of failed surfaces of the specimen confirmed that the crack front was uniform through the thickness of the specimen and that the surface measurements of crack length provide sufficiently accurate estimates of the rates of fatigue crack growth through the specimen thickness.

As shown later, a major factor promoting the growth of fatigue cracks from notches subjected to cyclic compression is the possible generation of residual tensile stresses. If localized residual tensile stresses are responsible for fatigue fracture under far-field cyclic compression, the mechanisms of compression fatigue crack growth would be expected to exhibit some similarity to those of tension fatigue. Indeed, such similarities have been documented for fatigue cracks in metallic materials. For this reason, fatigue crack growth tests were also conducted in the present work on HDPE under fully tensile cyclic loads at a load ratio $R = 0.1$ and frequency $\nu = 4$ Hz (sinusoidal waveform) in the laboratory environment using the compact specimen geometry. For the tensile fatigue tests, the initial crack length to the specimen width ratio was at least 0.31 before data were collected.

Although the principal focus of this study was HDPE, a limited number of compression fatigue experiments were also conducted on polystyrene in an attempt to demonstrate the generality of the cyclic compression mechanism in polymers. Furthermore, because polystyrene is known to be highly susceptible to craze formation, some critical issues pertaining to the mechanisms of compression fatigue fracture could also be addressed. For example, it is known that crazes are formed in a direction normal to the maximum principal stress axis. Therefore, if it can be experimentally demonstrated that craze formation occurs in cyclic compression along the Mode I fatigue crack (i.e. in a direction normal to the far-field compression axis), it is a very compelling evidence for the argument that residual tensile stresses are induced at the tip of the notch. The polystyrene polymer was obtained from Dow Chemical Co., Midland, MI. The polymer is amorphous; its weight-average molecular weight, M_W, is 240 000 and its number-average molecular weight, M_n, is 86 000 (i.e. polydispersity of 2.8). The specimens used for compression fatigue testing were of the SEN geometry. The specimen geometry and dimensions of the SEN specimen are shown schematically in Fig. 1a. The specimen dimensions for this case are length $W = 19.05$ mm, height $2H = 19.05$ mm, notch length $a_0 = 5.715$ mm, thickness $B = 3.17$ mm, notch root radius $\rho = 0.127$ mm, and notch tip angle $\theta = 45°$.

3. Results

3.1. Compression fatigue crack growth in HDPE

The first objective of this investigation was to determine if fatigue cracks could initiate and propagate in HDPE by the application of fully compressive far-field

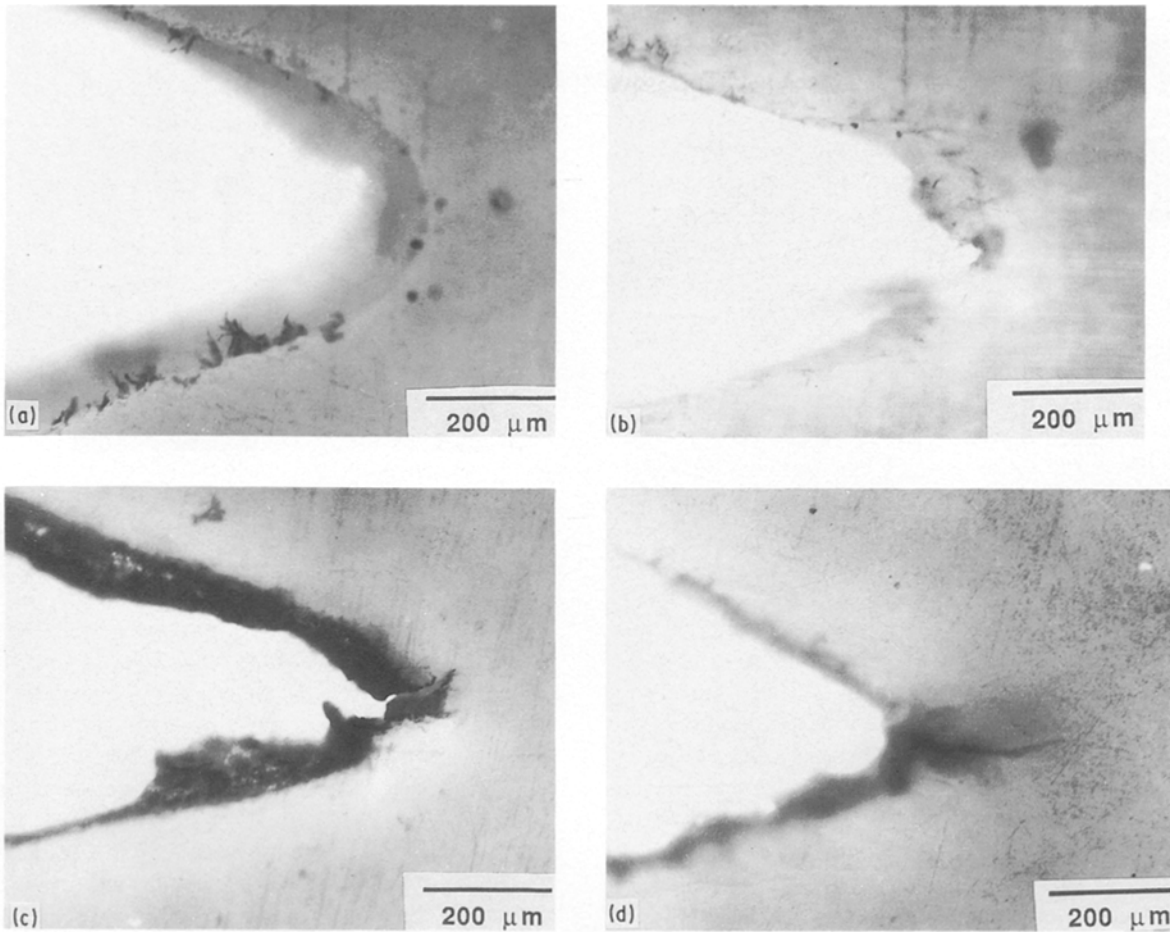

Figure 2 Sequence of optical micrographs of a Mode I fatigue crack which propagated from the root of the notch in the compact specimen after (a) 0, (b) 1, (c) 10 000 and (d) 2 500 000 cycles of uniaxial compression loading.

cyclic loads. Fig. 2a–d shows a sequence of optical micrographs of a Mode I fatigue crack at the root of the notch observed in the pin-loaded compact specimen after 0, 1, 10 000 and 2 500 000 cycles of uniaxial compression loading. These micrographs reveal the evolution of damage at the notch-tip with the imposition of compression cycles and the initiation of fatigue crack propagation perpendicular to the compression axis along the plane of the notch. A similar crack growth behaviour was also observed in the SEN specimen geometry. The fatigue cracks propagate at a progressively slower rate and arrest completely after a certain "saturation growth distance", a^* (see the schematic drawing in Fig. 3). Fig. 4a is a scanning electron micrograph of the fatigue crack profile (of the same compact specimen as in Fig. 2) after saturation of crack propagation. Fig. 4b is a scanning electron micrograph which depicts the self-arrested compression fatigue crack profile in the uniformly loaded SEN specimen. The saturation crack length, a^*, load ratio, R, loads used for crack initiation, P_{max} and P_{min}, and the nominal stress amplitude $|\Delta\sigma|$ for the compression fatigue tests are given in Table I. For the conditions of the experiments shown in this table, the through-thickness fatigue cracks propagated over a distance of up to 0.32 mm. It should be noted that small differences in the notch-root radius or notch-tip angle among the different test specimens can lead to large variations in the local stress in the immediate vicinity

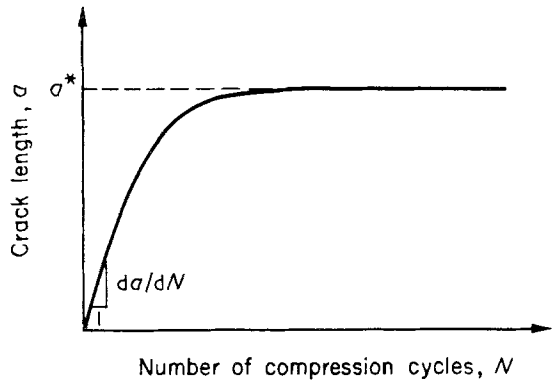

Figure 3 Schematic showing crack length, a (measured from the notch tip) as a function of the number of compression cycles, N.

of the notch-tip. Furthermore, as discussed later, the frictional contact of the faces of the incipient crack (which is a strong function of the microscopic roughness of the crack front) can have a marked effect on its rate of growth. In view of these complicating factors, it is not feasible to pinpoint precisely the origin of the differences in a^* for the various test conditions listed in Table I.

These fatigue cracks appear macroscopically similar to Mode I compression fatigue cracks observed in both brittle [10, 11] and ductile [1–7] crystalline solids (see Section 4). Although the macroscopic fatigue behaviour of crystalline and non-crystalline

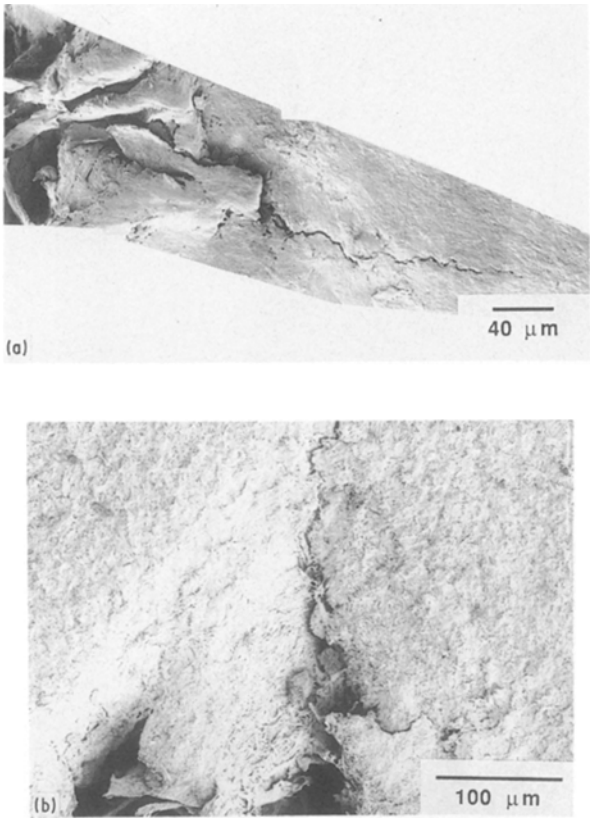

Figure 4 Scanning electron micrographs of (a) a fatigue crack profile in compact specimen after saturation of crack propagation, and (b) a self-arrested compression fatigue crack profile in an SEN specimen.

TABLE I Results of compression fatigue crack growth in high-density polyethylene

Test no.	Specimen	P_{min} (N)	P_{max} (N)	R	a^a (mm)
1	Compact	− 267	− 13	20	0.28
2	Compact	− 222	− 11	20	0.19
3	Compact	− 267	− 13	20	0.32
4	SEN[a]	− 1824 [21.9]	− 91 [1.1]	20	0.21
5	SEN[a]	− 1223 [14.7]	− 61 [0.7]	20	0.29
6	SEN[a]	− 1370 [16.5]	− 68 [0.8]	20	0.21

[a] The numbers within the square brackets for the SEN specimens show the nominal values of the maximum and minimum stress (MPa) applied uniformly on the top and bottom surfaces.

materials are similar in this respect, the underlying micromechanisms are different. Fig. 5a is a scanning electron micrograph taken ahead of the tip of the fatigue crack in the compact specimen of HDPE. This micrograph shows that the fatigue crack is discontinuous on the microscopic scale and that permanent damage in the form of microscopic cracking is induced at the crack tip. The orientation of the view shown in this photograph is such that the flaws are oriented normal to the compression axis. Fig. 5b is a scanning electron micrograph of the fibrils along the crack (parallel to the compression axis) in the uniformly loaded SEN specimen.

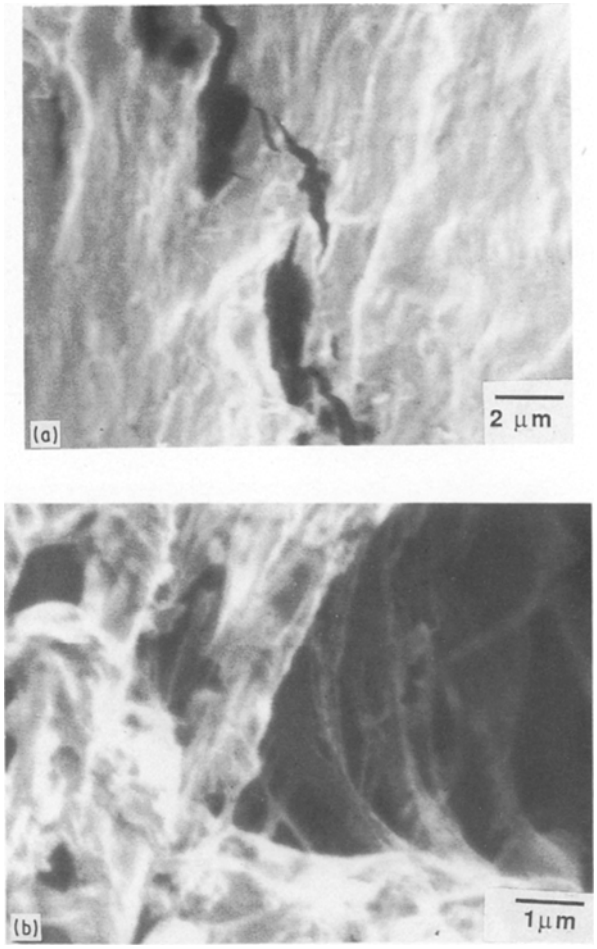

Figure 5 Scanning electron micrographs (a) taken near the tip of the fatigue crack showing the discontinuous crack growth; (b) of fibrils along the crack wake which are oriented parallel to the compression axis.

3.2. Comparisons of cyclic tension and cyclic compression fractures

As noted earlier, certain tensile fatigue tests were also conducted on HDPE to compare and contrast the fatigue mechanisms under cyclic tension with those seen under far-field cyclic compression. Fig. 6 shows the tensile fatigue crack growth rates, da/dN, as a function of the stress intensity factor range, ΔK, for a compact tension specimen subjected to uniaxial cyclic tensile loads. The relationship between the crack growth rate, da/dN, and the applied stress intensity range, ΔK, is similar to that found in crystalline solids. Specifically, a Paris power law relationship of the form $da/dN = C(\Delta K)^m$ is observed with $C = 1.74 \times 10^{-7}$ m/cycle $(\text{MPa m}^{1/2})^{-m}$ and $m = 4$. Fig. 7 shows the fatigue crack growth behaviour of the HDPE studied in this work along with the fatigue characteristics of other HDPE materials of different molecular weights (between $M_W = 70\,000$ and 200 000) reported in Hertzberg and Manson [14]. It can be seen that the data from Fig. 6 lie between the $M_W = 70\,000$ and the $M_W = 200\,000$ data, as would be expected for our HDPE polymer with $M_W = 91\,000$.

The comparison of tension fatigue and compression fatigue mechanisms was made using scanning electron

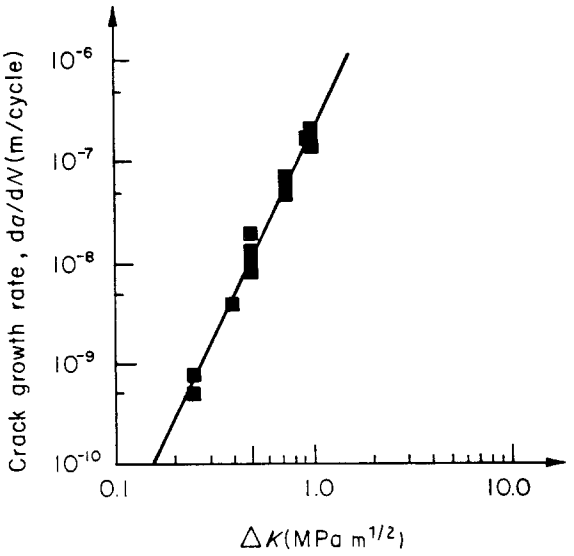

Figure 6 Tensile fatigue crack growth behaviour of HDPE. $R = 0.1$; $\nu = 4$ Hz.

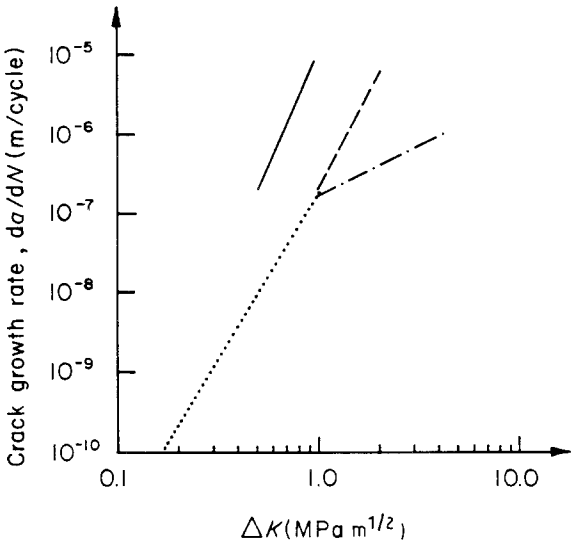

Figure 7 Tensile fatigue crack growth behaviour of HDPE as a function of molecular weight. The data for $M_w = 91\,000$ corresponds to this study; the remaining data were taken from [14]. M_w: (—) 45 000, (– – –) 70 000, (···) 91 000, (–·–) 200 000.

fractography. The fracture surfaces, created by overloading the specimens, were first studied optically and then sputter-coated for SEM analysis. For the purposes of comparing the growth kinetics of fatigue cracks advanced in cyclic compression and cyclic tension on a common scale, it is reasonable to suppose that identical rates of fatigue crack growth will be caused by identical values of "effective driving force", i.e. an effective stress intensity factor range at the crack tip. Consequently, the initial rates of growth, da/dN, of compression fatigue cracks were determined from the slopes of the crack growth curve (Fig. 4). The scanning electron micrographs corresponding to fracture at this growth rate were then compared with those for an identical growth rate in tension–tension fatigue. Fig. 8a and b show an example of a pair of scanning electron micrographs representing fracture at identical growth rates. Fig. 8a corresponds to compression fatigue loading at a growth rate of 1.1

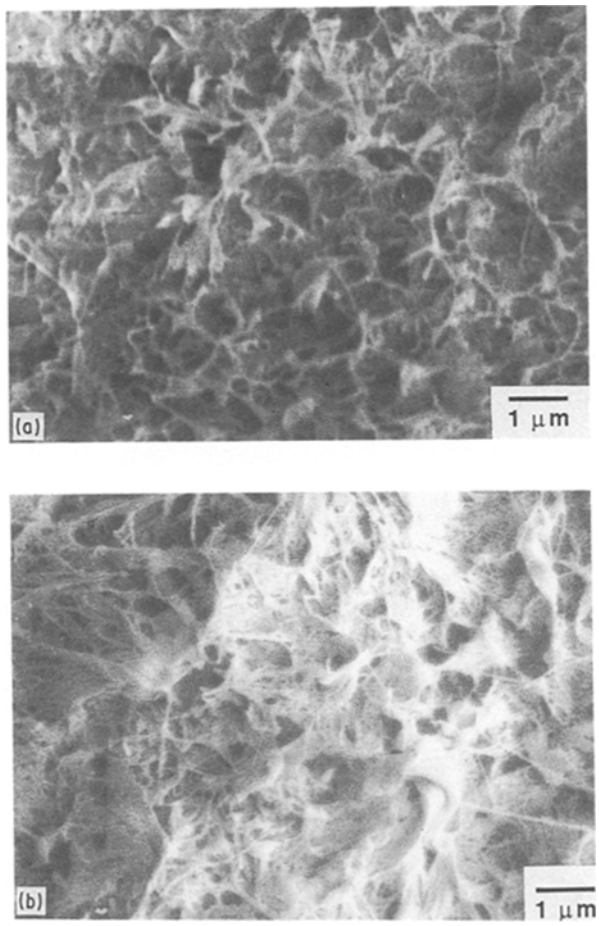

Figure 8 A pair of scanning electron micrographs showing the microscopic fracture mode under (a) far-field cyclic compression, and (b) far-field cyclic tension at comparable growth rates in HDPE.

$\times 10^{-8}$ m/cycle and Fig. 8b corresponds to a similar growth rate in tension fatigue (for which the nominal $\Delta K = 0.5$ MPa m$^{1/2}$). The similarity of fracture surface features is evident in the two cases.

3.3. Compression fatigue in polystyrene

The nucleation and growth of a fatigue crack in a notched plate of polystyrene are illustrated with the micrographs in Fig. 9a–c. Note the presence of damage directly ahead of the notch-tip in Fig. 9a which was taken after 15 000 compression cycles. The progressive increase in the length of the fatigue crack with increasing number of compression cycles is seen from the micrographs in Fig. 9b and c which were taken after 20 000 and 50 000 compression cycles, respectively. Note also the formation of a craze zone directly ahead of the fatigue crack; the craze is oriented normal to the far-field compression axis. Because crazes form along planes oriented normal to the direction of a (local) tensile stress, Fig. 9 also implies that residual tensile stresses are generated ahead of the crack even if the far-field loading is fully in compression. The fatigue crack in polystyrene advances over a total distance of 0.52 mm before arresting. Another important aspect of compression fatigue fracture in polystyrene is that crack growth is highly discontinuous. For the conditions of the experiments, the fatigue crack remains dormant typically for about 5000

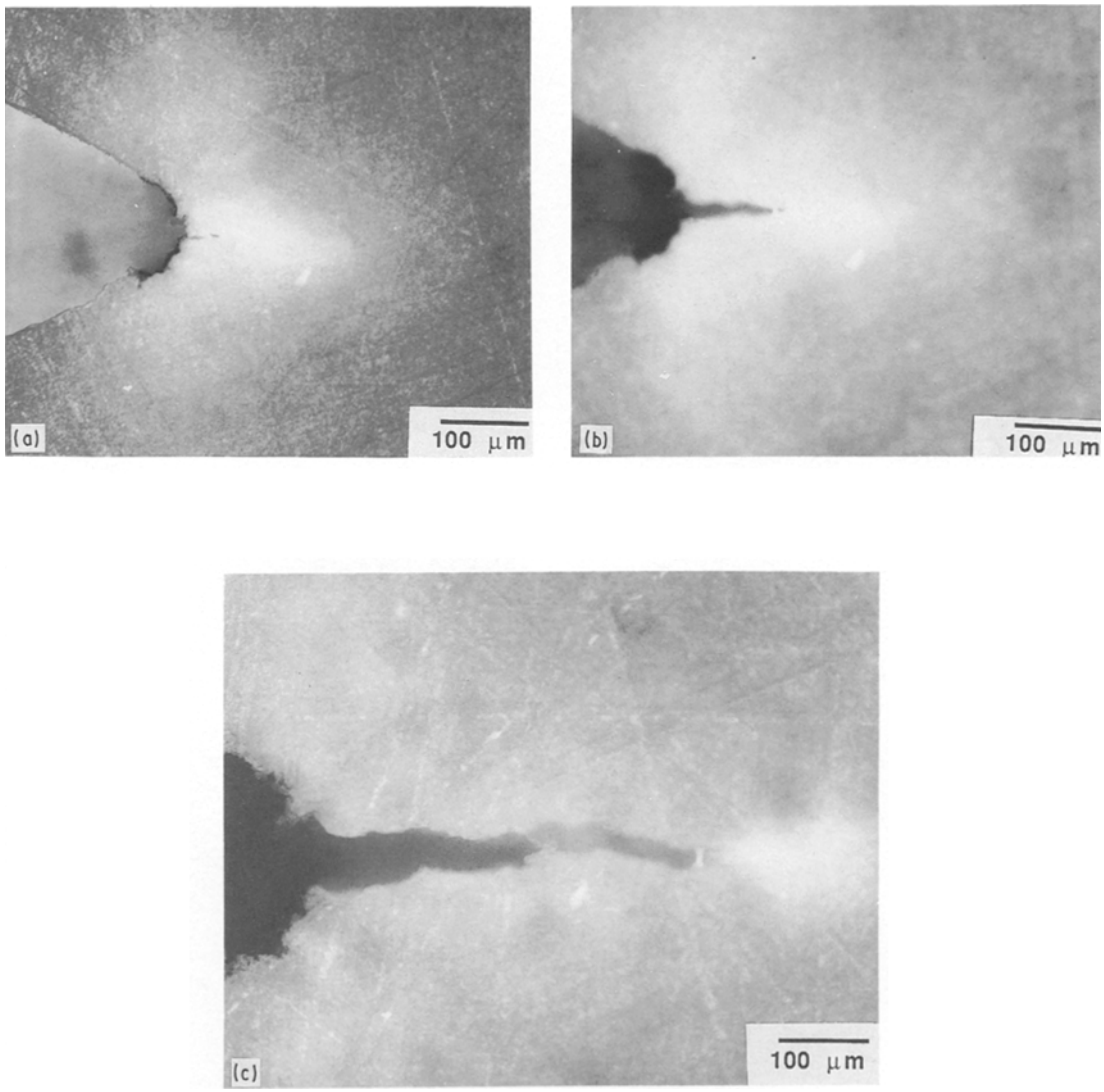

Figure 9 Nucleation and growth of a Mode I fatigue crack from the notch tip in polystyrene subjected to cyclic compression. (a) 15 000 cycles (b) 20 000 cycles and (c) 50 000 cycles. Note the formation of a craze damage zone ahead of the crack tip.

fatigue cycles (in the early stages of fatigue) following which there is a sudden burst of crack growth. This abrupt crack extension is apparently associated with cracking along the length of the craze; possibly aided by buckling within the craze (e.g. [14, 15]). (The discontinuous fracture process is also evident from the micrographs shown in Fig. 9 where the growth rates are not directly related to the number of imposed compression cycles.) It is interesting to draw an analogy between the discontinuous fatigue fracture of polystyrene in cyclic compression and the discontinuous growth of tensile fatigue cracks in crazeable polymers (e.g. [16–20]). A comprehensive review of crazing in monotonic and cyclic fractures can be found in [21, 22]. The size of the craze zone and the extent of sudden jump of the tensile fatigue crack (i.e. discontinuous growth) have been correlated with Dugdale-type models which reveal that the craze zone size is proportional to the square of the maximum stress intensity factor range and inversely proportional to the square of the craze strength [17–20]. It is, however, difficult to make such quantitative predictions for cyclic compression fracture where the effective stress intensity factor due to the residual tensile field cannot be quantified from the present experiments alone.

4. Discussion

The present study has provided clear experimental evidence for the occurrence of stable fatigue crack growth in polymeric materials subjected to fully compressive cyclic loads. The cracks grow at a decelerating rate before arresting. The macroscopic mode of compression fatigue fracture (i.e. Mode I) as well as the growth kinetics of compression fatigue described in this study are similar to the trends seen in metallic and ceramic materials. Fig. 10a and b show examples of Mode I fatigue crack growth under far-field cyclic compression in a metal–matrix composite comprising Al–3.5 wt % Cu alloy reinforced with 20 vol % SiC particulates and in a polycrystalline alumina ceramic (average grain size = 18 μm), respectively. Note the similarity of crack growth in these two figures to that seen in Figs 2 and 9.

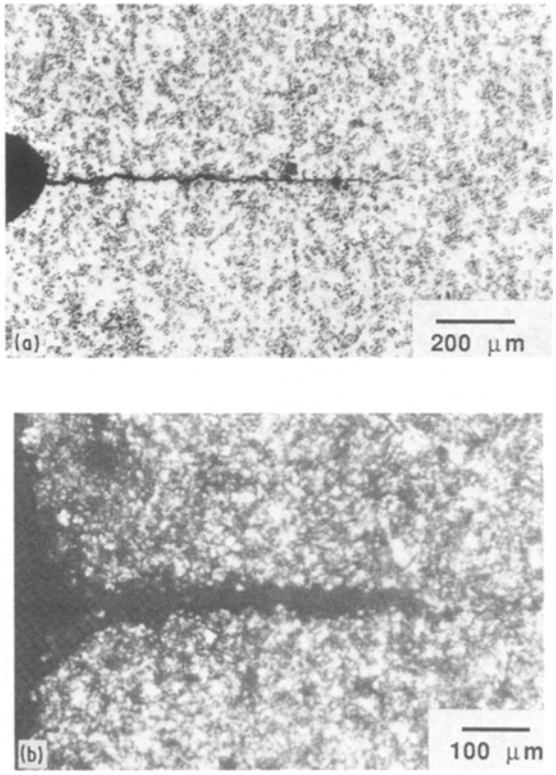

Figure 10 Examples of Mode I fatigue crack growth under fully compressive cyclic loads in (a) Al–3.5 wt % Cu alloy reinforced with 20 vol % SiC particles, and (b) polycrystalline alumina.

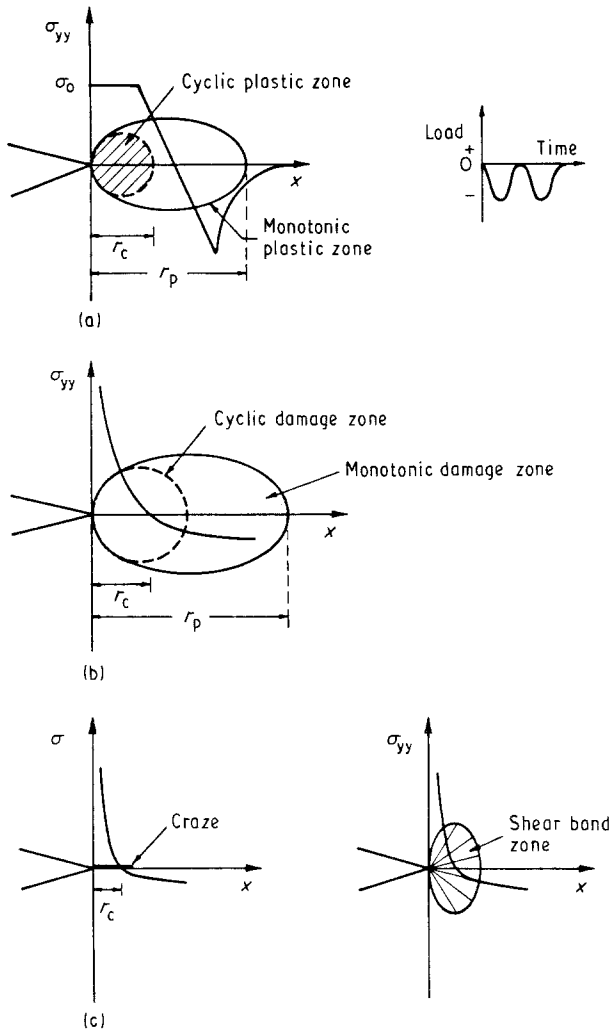

Figure 11 Schematic representation of the generation of residual tensile stresses at the notch tip upon unloading from the maximum far-field compressive load. (a) Elastic–perfectly plastic solid, (b) microcracking brittle solid, and (c) polymeric material.

As alluded to in Section 1, the initiation and growth of a fatigue crack from a notch under fully compressive cyclic loads is a consequence of the development of a zone of residual tensile stresses upon unloading from the maximum far-field compressive load. It is a well known result that for an elastic–perfectly plastic solid containing a non-closing sharp notch and subjected to cyclic compressive stresses, the zone of residual tensile stresses (of magnitude equal to the flow strength in tension) is created over a distance which is of the order of the cyclic plastic zone size (which is approximately one-fourth the size of the monotonic plastic zone created at the peak far-field compressive stress) (e.g. [23, 24]). This process is schematically illustrated in Fig. 11a.

If, instead of plastic flow, the material exhibits a different mode of permanent deformation, such as microcracking, the generation of residual tensile stresses can still occur because of the creation of a cyclic damage zone. On the basis of experimental observations of distributed microcracking ahead of the notches in alumina ceramics subjected to cyclic compression, Suresh and Brockenbrough [11] conducted detailed finite element simulations of near-tip stresses at notches. Their analysis revealed that, when permanent strains are retained within the notch tip damage zone, large residual tensile stresses were created. The tensile stress field decays precipitously with distance ahead of the notch tip. Because residual stresses are self-equilibrating, tensile residual stresses in the immediate vicinity of the notch tip must be counterbalanced by compressive residual stresses in the regions away from the notch tip. Fig. 11b schematically shows the variation of the normal stress, σ_{yy}, as a function of the distance ahead of the notch tip in a microcracking brittle solid cycled in compression. It is interesting to note that some earlier workers have observed craze formation ahead of circular holes in PMMA on unloading from a single monotonic compressive load [25]. Although crack initiation under cyclic compression was not studied and micrographs not provided, the results of Reference 25 support the interpretations of the present work.

In the case of polymeric materials, permanent deformation ahead of the notch-tip region is induced by crazing, shear flow, or a combination of the two mechanisms. Unloading from a far-field compressive stress, therefore, results in residual tensile stresses in much the same way as for fully crystalline solids; see Fig. 11c. A definitive experimental support for the argument that local residual tensile stresses in the notch-tip region cause stable Mode I fatigue fracture under far-field cyclic compression is also found from the results shown for polystyrene. Craze formation occurs ahead of the advancing fatigue crack, with the craze oriented along the plane of the crack and in a direction perpendicular to the cyclic compression loading axis. This feature clearly implies that tensile

residual stresses must act on the material at the tip of the notch in order for the craze to form.

The compression fatigue cracks decelerate because an increase in the length of the fatigue crack leads to an increase in the level of crack closure under far-field cyclic compression; this also results in an exhaustion of the residual tensile stress field. With increasing crack length, the fraction of the loading cycle during which the crack remains open progressively diminishes [24]. Once a certain saturation crack length is reached, the level of the residual tensile field left at the crack tip is insufficient to advance the crack against the imposition of the far-field cyclic compressive load. It should be noted that it is the tensile mode of fracture which is responsible for fracture on a local scale even if the far-field cyclic loading is in compression. Therefore, it is not surprising that the microscopic mechanisms of fatigue fracture in cyclic compression exhibit a similarity to those seen in cyclic tension.

5. Conclusions

1. It is demonstrated that the application of fully compressive cyclic loads to high-density polyethylene and polystyrene with stress concentrations can lead to progressively decelerating fatigue crack growth in a direction macroscopically normal to the compression axis.

2. The macroscopic fatigue behaviour of these semicrystalline polymers is similar to that observed in metals, ceramics and inorganic composites.

3. The apparent similarity between the notch tip tensile zones for both brittle and ductile solids is explained by the fact that deformation at the notch tip creates permanent strains upon unloading from the far-field compressive stress, thereby forming a zone of residual tension at the notch tip.

4. Evidence for the existence of a local residual tensile field at the notch tip is provided with the aid of micrographs which reveal craze formation along the plane of the notch. Fracture in cyclic compression (in polystyrene) is also highly discontinuous. The crack growth behaviour exhibits periodic crack arrest followed by a burst of crack extension, ostensibly in connection with fracture along the craze. The intermittent growth process is analogous to the formation of discontinuous growth bands during the tension fatigue of many engineering plastics which exhibit crazing.

Acknowledgements

This work was supported by the Office of Naval Research under Contract no. N00014-89-J-3099. The authors thank Dr A. K. Vasudevan for his helpful discussions, Dr T. Juska for supplying the high-density polyethylene, Mr C. Bull for his experimental assistance and Ms Y. Sugimura for providing Fig. 10a.

References

1. R. P. HUBBARD, *J. Basic Engng Trans. ASME* **91** (1969) 625.
2. H. SAAL, *ibid.* **94** (1972) 243.
3. C. N. REID, K. WILLIAMS and R. HERMANN, *Fat. Engng Mater. Struct.* **1** (1979) 267.
4. N. FLECK, C. S. SHIN and R. A. SMITH, *Engng Fract. Mech.* **21** (1985) 173.
5. S. SURESH, *ibid.* **21** (1985) 453.
6. T. CHRISTMAN and S. SURESH, *ibid.* **23** (1986) 953.
7. R. PIPPAN, *Fat. Engng Mater. Struct.* **9** (1987) 319.
8. T. H. TOPPER and M. T. YU, *Int. J. Fat.* **7** (1985) 159.
9. P. B. ASWATH, S. SURESH, D. K. HOLM and A. F. BLOM, *J. Engng Mater. Tech. Trans. ASME* **110** (1988) 278.
10. L. EWART and S. SURESH, *J. Mater. Sci.* **22** (1987) 1173.
11. S. SURESH and J. R. BROCKENBROUGH, *Acta Metall.* **36** (1988) 1455.
12. S. MORRIS, PhD thesis, University of Nottingham (1970).
13. S. SURESH and L. PRUITT, in "Deformation, Yield and Fracture of Polymers", Proc. 8th Int. Conf., Churchill College, Cambridge University, April 1991, edited by R. J. Young (The Plastics and Rubber Institute, London, 1991) p. 32-1.
14. P. J. MILLS, H. R. BROWN and E. J. KRAMER, *J. Mater. Sci.* **20** (1985) 4413.
15. H. R. BROWN, E. J. KRAMER and K. A. BUBECK, *J. Poly. Sci., Poly. Phys. B.* **25** (1987) 1765.
16. R. W. HERTZBERG and J. A. MANSON, "Fatigue of Engineering Plastics" (Academic Press, New York, 1980).
17. J. P. ELINCK, J. C. BAUWENS and G. HOMÉS, *Int. J. Fract.* **7** (1971) 277.
18. M. D. SKIBO, R. W. HERTZBERG, J. A. MANSON and S. KIM, *J. Mater. Sci.* **12** (1977) 531.
19. L. KÖNCZÖL, M. G. SCHINCKER and W. DÖLL, *J. Mater. Sci.* **19** (1984) 1605.
20. W. DÖLL and L. KÖNCZÖL, *Adv. Poly. Sci.* **91/92** (1990) 138.
21. E. J. KRAMER and L. L. BERGER, *ibid.* **91/92** (1990) 1.
22. J. SAUER and M. HARA, *ibid.* **91/92** (1990) 69.
23. S. SURESH, *Int. J. Fract.* **42** (1990) 41.
24. S. SURESH, "Fatigue of Materials" (Cambridge University Press, 1991).
25. L. BEVEN, *J. Mater. Sci. Lett.* **13** (1978) 216.

Received 23 November 1990
and accepted 10 April 1991